Correlation of local Jahn-Teller distortions to the magnetic/conductive states of $La_{1-x}Sr_xCoO_3$

Despina Louca, J. L. Sarrao, J. D. Thompson, H. Röder, and G. H. Kwei
Los Alamos National Laboratory, Los Alamos, New Mexico 87545
(Received 24 June 1999)

By relating the structural changes measured using the pair density function analysis of pulsed neutron data for $LaCoO_3$, we provide evidence for the evolution of the magnetic state with temperature, from the low-spin state to partial occupation of the intermediate spin (IS) and to the high-spin states. It can also be inferred that the coupling strength of the lattice to the e_g electronic states is temperature dependent. The introduction of carriers in $La_{1-x}Sr_xCoO_3$ stabilizes the IS states, populated at a rate proportional to the overall carrier density. The transition to the metallic state with doping is accompanied by distortions of the lattice at short length scales, which is compatible with the picture of a Jahn-Teller glass. [S0163-1829(99)05538-1]

The spin transitions in cobalt perovskites induced by temperature and the doping of charge carriers are rather unusual and are as controversial today as when they were first proposed.[1,2] The ground-state electronic spin configuration of Co in the parent compound $LaCoO_3$ is the low-spin (LS) $(t_{2g}^6 e_g^0)$ state. A broad transition in the magnetic susceptibility observed at ~100 K (Ref. 3) corresponds to the thermal activation of an excited state which could be either a high-spin (HS) $(t_{2g}^4 e_g^2)$ or an intermediate-spin (IS) $(t_{2g}^5 e_g^1)$ configuration. Several studies provided evidence to support one transition type over the other but the issue still remains unresolved[2–5] with the majority of new results pointing towards the sequence LS→IS→HS with increasing temperature.

With doping, one observes a similar evolution in the magnetic and transport properties of $La_{1-x}Sr_xCoO_3$ as in the manganites.[5,6] The competing mechanisms for activation, driven thermally and/or by doping, result in the establishment of ferromagnetic Co-Co coupling through the creation of either IS or HS sites. The fact that the cobalt perovskites do not exhibit colossal magnetoresistance (CMR) in spite of their high metallic conductivity suggests that fundamental differences in the strength of the spin to charge and lattice coupling between the two systems exists.[7]

The magnetic phase diagram of $La_{1-x}Sr_xCoO_3$ inferred from our magnetic susceptibility data is shown in Fig. 1(a) and the $\chi(T)$ for $LaCoO_3$ in Fig. 1(b). Pure $LaCoO_3$ is nonmagnetic at the lowest measured temperature, while a smooth ''transition'' is observed at ~100 K as reported in the literature.[3,7,8] This transition is a result of thermal activation from the LS to a higher-spin state. Above 100 K, the curve shows Curie-Weiss behavior. With small amounts of Sr, $\chi(T)$ is similar to that of the undoped material.[7] Above 5% Sr doping, a spin-glass transition T_G is observed and above $x \geqslant 0.18$, $La_{1-x}Sr_xCoO_3$ becomes a ferromagnetic (FM) metal. A reentrant magnetic state is observed from $x = 0.15$ to 0.18, where the transition is not clearly ferromagnetic. This is an unusual spin glass, probably caused by variable long-range interactions and not by alternating (frustrated) short-ranged forces.[9]

Raman studies of the electronic structure for the $La_{1-x}Sr_xCoO_3$ system alluded to the fact that the observed spin fluctuations would be consistent with distortions in the local structure reflecting the type of transition.[7] While these are indirect observations of the local structure, we show, using the pair density function (PDF) analysis of neutron diffraction data, the type and size of local distortions occurring in this system. In the study of $LaCoO_3$ below the transition, the coupling of lattice to electronic states gives rise in a one-to-one correspondence with the activation of simple e_g Jahn-Teller (JT-) active IS states. Above the transition, the reduction of the IS JT distortions brought about by the increased population to the HS state results in a mixed spin-state configuration with the possible presence of all three states. Doping results in an even stronger e_g-lattice coupling,

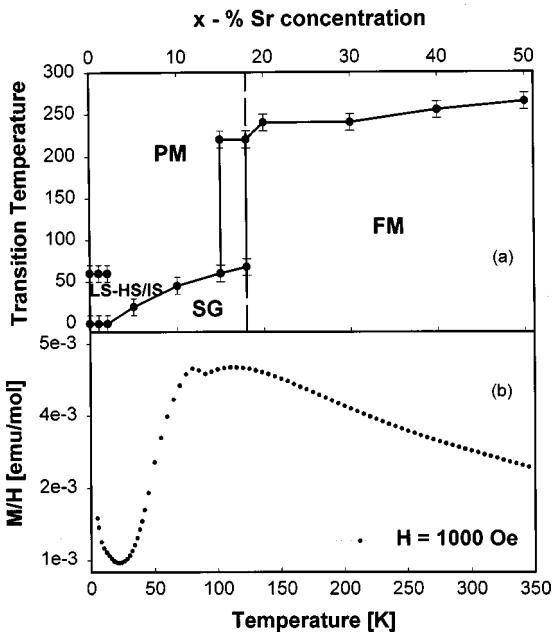

FIG. 1. (a) The magnetic phase diagram in zero-field measurements. At very low doping, the system is nonmagnetic; it slowly transforms into a spin glass (SG), then to a spin-cluster-glass phase, and then becomes ferromagnetic (FM). (b) The magnetic susceptibility of $LaCoO_3$. The transition observed near 100 K is due to the conversion of diamagnetic low-spin Co ions to the IS state. The upturn observed in $\chi(T)$ below 30 K and the little dip at ~90 K are due to extrinsic effects as discussed in Ref. 8.

 ©1999 The American Physical Society

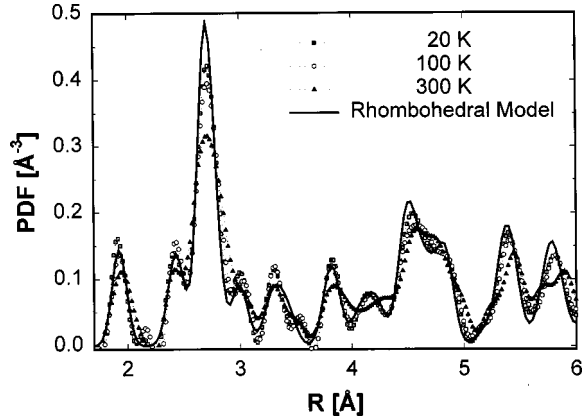

FIG. 2. The PDF of $LaCoO_3$ at 20, 100, and 300 K. At 20 K, the measured PDF agrees quite well with the PDF calculated for the $R\bar{3}C$ model for this compound. At 100 K, the long Co-O bonds appear. By 300 K, significant deviations are observed locally from the average crystal structure.

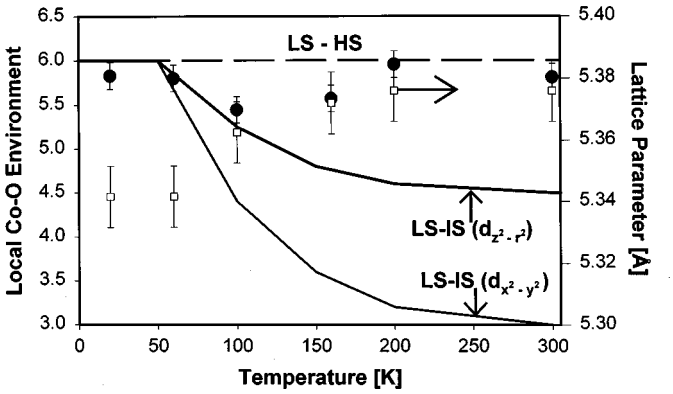

FIG. 3. The local coordination number of Co as a function of temperature for $LaCoO_3$. The distortions strongly couple to the LS-IS transition up to 100 K where the expected change in the local environment is taken from Ref. 14 (solid lines). Above 100 K, a mixed spin state is present, gradually converting to the HS configuration (Ref. 16). The lattice parameter (squares) changes with temperature in the same way as the local Co-O environment.

giving rise to typical JT phenomena. In addition, the T_{2g} rhombohedral distortions become less cooperative and the local lattice becomes glassy with the transition to the metallic state, where the lattice distortions most likely become dynamic in nature.

The ceramic samples were prepared by the standard solid-state reaction method from La_2O_3, $SrCoO_3$, and Co_3O_4, fired several times at 1100 °C with a final firing at 1300 °C in air for 1 day. The pure sample was additionally annealed in nitrogen at 900 °C for 1 day to ensure stoichiometric oxygen content. The neutron diffraction data were collected using the Glass Liquid and Amorphous Diffractometer (GLAD) at the Intense Pulsed Neutron Source (IPNS). Data were collected from 300 K down to 15 K and were all corrected for instrumental background, absorption, incoherent scattering, and inelastic and multiple scattering.[10] The PDF $\rho(r)$ obtained through a Fourier transform of the $S(Q)$, which is determined up to high momentum transfers $Q=33\,\text{Å}^{-1}$, is a real-space representation of the atomic density correlations. The PDF analysis provides direct information with regard to the local structure,[10] and it has been previously used successfully to determine the local structure of manganites.[11]

The electronic ground state of the nonmagnetic insulator $LaCoO_3$ has the t_{2g}^6 configuration at 0 K. On average, the crystal is rhombohedral with $R\bar{3}C$ symmetry. The structure has a relatively large distortion angle α along the [111] direction of 10.3° [12] which originates from the rotation of oxygen octahedra. With the e_g orbitals empty, the directional Coulomb repulsion between the Co and O atoms is minimal. Structurally, the CoO_6 octahedra are almost symmetric and the Co-O bond distances are quite similar. This is represented by a single Co-O peak at 1.915 Å, which is the first peak in the PDF for this compound, at 20 K (squares) (Fig. 2). The model PDF calculated for the $R\bar{3}C$ structure for $LaCoO_3$ (solid line) agrees quite well with the experimentally determined PDF. By 300 K (triangles), the PDF peaks height decrease significantly. This partly originates from the increase in the amplitude of atomic thermal vibrations. However, the shapes of the PDF peaks show additional deviations from the ideal crystallographic structure, while the average crystal structure remains rhombohedral.

The nature of the transition from the LS state was investigated by studying the temperature dependence of the Co-O bond. As the e_g orbital is thermally populated, the CoO_6 octahedral environment is locally modified depending on the coupling strength of the e_g to the lattice. In the weak-coupling limit, an IS transition cannot be distinguished from a HS state because the e_g-lattice interactions and the subsequent atomic distortions are small. In the strong-coupling regime, however, it is feasible to distinguish one transition type from the other as the IS state has a single occupancy of the e_g orbitals resulting in a JT-active mode (as in Mn^{3+}) whereas the HS state is not JT active. The IS interactions can result in cooperative JT phenomena giving rise to significant structural distortions. In the IS scenario, population of the e_g orbitals [with an activation energy of 257 K (Ref. 14)] will be reflected as a split in the Co-O distances to short and long. Integration of the area under the first PDF peak provides the number of nearest neighbors with respect to Co,[13] and in an ideal octahedral environment without any distortions, it is 6, the coordination number. The ratio of short and long bonds will depend on the orbital that actually becomes occupied. On the other hand, the HS transition produces distortions that are of the breathing-mode type, $^5T_{2g}$, associated with small displacements of the oxygen atoms[15] and with very little splitting of the Co-O bond lengths. With these criteria in mind, the lines of Fig. 3 represent the effective coordination resulting from the two types of transitions as determined from the population rate per activation state as a function of temperature in Ref. 14. As can be seen, the Co-O local environment determined from the PDF is reduced from 6 (the ideal case) with increasing temperature. The observed change corresponds to a LS→IS transition up to 100 K, with $d_{z^2-r^2}$ orbital occupancy. In the case of $d_{x^2-y^2}$ occupancy, the rate of change of the Co-O environment would have been a lot more pronounced. The percent of occupied IS states at this temperature is about 40% with the rest of the ions still in the LS configuration. The long Co-O bonds due to the local JT distortions of the IS state sites are represented by a secondary Co-O peak ~2.16 Å, seen in the PDF determined at

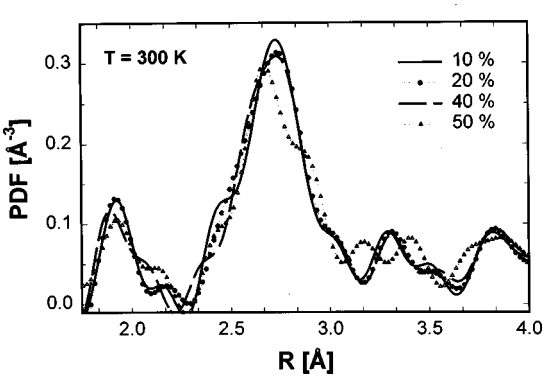

FIG. 4. The local atomic structure at $x=0.1$, 0.2, 0.4, and 0.5 at 300 K. Note the development of the peak of the long Co-O bonds at 2.13 Å with doping that is absent in $LaCoO_3$ at this temperature. This is due to the formation of the JT-active IS states, where the peak gets stronger as the concentration is increased.

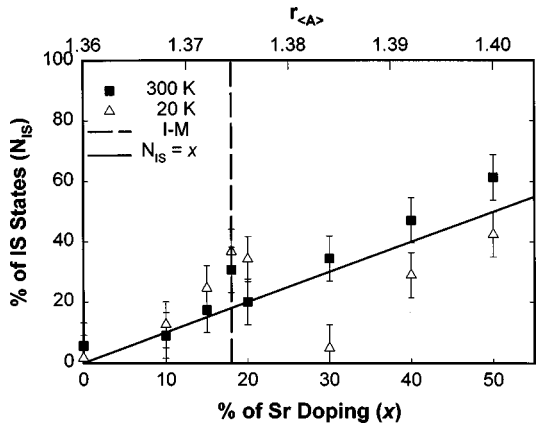

FIG. 5. The percent of IS sites formed as a function of doping (also plotted as a function of the ionic radius $r_{\langle \text{Å} \rangle}$) at 20 and 300 K. At 300 K, the number of IS sites is linearly proportional to x where the system is a paramagnetic insulator. At 20 K, a break-in of the slope is observed around the *I-M* transition due to the formation of the JT glass state in the metallic phase.

100 K (Fig. 2), but because it is small, at the level of noise, its amplitude is not well determined. For this reason, the integration is carried only up to the end of the first peak. Deviations from the LS-IS strong-coupling limit are observed from 100 to 300 K. The increase in the full width at half maximum (FWHM) of the Co-O peak at 300 K in Fig. 2 reflects the expansion of the unit-cell volume due to activation of the HS state.[16] This could additionally suggest that the charge-to-lattice coupling changes with temperature due to the increase in the charge mobility, thus modifying the effective lattice distortions. Also shown in Fig. 3 is the temperature dependence of the lattice parameter which shows a similarity to the change in the local Co-O environment.

JT-active sites form also with doping. With the introduction of Co^{4+} sites through Sr doping, the local atomic structure changes (Fig. 4). While the average octahedral tilting angle is reduced with increased doping,[17] additional changes are seen in the local structure that cannot be accounted for assuming a global symmetry as the latter changes from rhombohedral to almost cubic. At 300 K, long Co-O bonds are clearly present in the PDF's from 10% of Sr onwards. Such a bond length arises from the formation of a stable IS state. The percentage of CoO_6 sites in the IS state is determined by calculating the number of short Co-O bonds (at 1.92 Å) (equation shown in Ref. 13) and subtracting that number from 6, the total number of bonds in the octahedron. This gives an estimate of the number of sites with a JT distortion (Fig. 5) which increases almost linearly with the charge concentration in the paramagnetic insulating phase, at a rate that is almost equal to x (solid line). This represents an increase in the population of the JT-active IS states due to the straightening of the Co-O-Co bonds with doping. Thus the transition occurs for different reasons with temperature (in $LaCoO_3$) than with doping. As a function of temperature, the higher entropy of the higher-spin states drives the transition, while as a function of doping, the increase in the average Co-O bond length reduces the crystal field splitting and shifts the balance towards the higher-spin states.

The nature of the structural distortions discussed up to this point are essentially static. However, in the metallic phase which commences at *18% of Sr and with cooling*, the distortions are consistent with the picture of a *JT glass state*. It is possible that the lattice coupling to the spin fluctuations and increased charge mobility give rise to dynamic distortions, reflected in the PDF data as a distortion in the Fourier transform of $S(Q)$. In time-of-flight (TOF) experiments, neutron detectors do not have energy resolution and both elastically and inelastically scattered neutrons are recorded at the detectors. The energy integration of $S(Q)$ (Ref. 18) has a finite cutoff, and the range varies depending on the angle bank. If high-energy modes are present in the system, they will appear in some banks and not in others, giving rise to a scattering-angle-dependent PDF. In the case where vibration modes are close to the energy cutoff, the Fourier transform is distorted.[18–20] This distortion depends upon the detector angle (i.e., momentum transfer), so variations in the PDF with the detector angle are an indication that the system has a local *dynamic* distortion. This is indeed the case for the

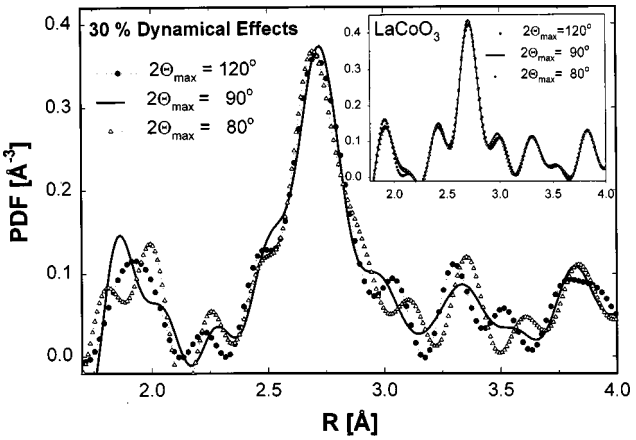

FIG. 6. The PDF at 20 K for the $x=0.30$ composition determined at different angles of diffraction. Data are integrated up to the 2θ values shown. Many changes are seen as the maximum diffraction angle is varied, suggesting that Q-dependent dynamic events occur in the structure. The energy of this local dynamic lattice mode is of the order of 20 meV (Refs. 19 and 20). The inset shows a typical case of no dynamics present in the system as in $LaCoO_3$ also at 20 K.

metallic compositions of this system ($x \geqslant 0.18$), as shown in Fig. 6 for $x=0.3$ as an example of how distorted the PDF can become, without any physical meaning associated with such variation of the structure with angle. In the absence of any localized dynamic mode, the PDF shows almost no variation with detector angle (see inset of Fig. 6 and Refs. 19 and 20). A similar effect has been observed in other systems, such as the CMR manganites, at the *M-I* transition with 15% of doping. This is clearly a phenomenon associated with dynamics in a system. The standard Placzek correction[21] used to correct for the presence of inelastic scattering events is inapplicable because it uses a ballistic approximation which does not work when strongly localized but dynamic lattice vibration modes are present.[19]

In a weak-coupling JT system, the effective long-range (elastic) interactions between JT sites can fluctuate in sign and magnitude.[22] The coupling to spin degrees of freedom may then frustrate the JT interactions and give rise to a spin-glass-like state.[22,23] One property of such a lattice glass is, as theoretical predictions indicate,[9] that the lattice is disordered at short scales and homogeneous at long scales. Such glassy behavior is not uncommon as previously thought as it can be widely observed in several ferroelectric systems. One would expect glassy (dynamical) behavior at the first peaks in the PDF, which is what is observed. It is interesting to note that the appearance of this phase coincides with the *I-M* phase transition. It may be speculated that the charge effectively decouples from the very slow lattice dynamics in the Bragg glass phase. The effective electron-phonon scattering becomes smaller and one obtains a ''normal'' metallic behavior.

In conclusion, the structural data provided in this work showed that the e_g-lattice coupling in $LaCoO_3$ changes with increased occupancy of the IS state with temperature, and evolution to the HS state at higher temperature. In $La_{1-x}Sr_xCoO_3$, the lattice couples more strongly to the spin fluctuations and stabilizes the JT-active IS state. The interaction of the lattice and charge dynamics in the metallic state gives rise to local dynamic distortions.

We acknowledge valuable discussions particularly with T. Egami, J. B. Goodenough, and S. Trugman. We especially thank J. A. Johnson for the help with the GLAD spectrometer. Work at the Los Alamos National Laboratory is performed under the auspices of the U.S. Department of Energy under Contract No. W-7405-Eng-36. The IPNS is supported by the U.S. Department of Energy, Division of Materials Sciences, under Contract No. W-31-109-Eng-38.

[1] G. H. Jonker and J. H. Van Santen, Physica (Amsterdam) **19**, 120 (1953).

[2] J. B. Goodenough, J. Phys. Chem. Solids **6**, 287 (1958); Mater. Res. Bull. **6**, 967 (1971).

[3] V. G. Bhide, D. S. Rajoria, C. N. R. Rao, G. R. Rao, and V. G. Jadhao, Phys. Rev. B **12**, 2832 (1975); M. Abbate, J. C. Fuggle, A. Fujimori, L. H. Tjeng, C. T. Chen, R. Potze, G. A. Sawatzky, H. Eisaki, and S. Uchida, Phys. Rev. B **47**, 16 124 (1993); K. Asai, O. Yokokura, N. Nishimori, H. Chou, J. M. Tranquada, G. Shirane, S. Higuchi, Y. Okajima, and K. Kohn, *ibid.* **50**, 3025 (1994); P. Ganguly, P. S. A. Kumar, P. N. Santhosh, and I. S. Mulla, J. Phys.: Condens. Matter **6**, 533 (1994); M. Itoh and I. Natori, J. Phys. Soc. Jpn. **64**, 970 (1995); S. Stølen, F. Gronvold, H. Brinks, T. Atake, and H. Mori, Phys. Rev. B **55**, 14 103 (1997); T. Saitoh, T. Mizokawa, A. Fujimori, M. Abbate, Y. Takeda, and M. Takano, *ibid.* **56**, 1290 (1997).

[4] P. M. Raccah and J. B. Goodenough, Phys. Rev. **155**, 932 (1967); J. Appl. Phys. **39**, 1209 (1968).

[5] S. Yamaguchi, H. Taniguchi, H. Takagi, T. Arima, and Y. Tokura, J. Phys. Soc. Jpn. **64**, 1885 (1995).

[6] M. R. Ibarra, R. Mahendiran, C. Marquina, B. Garcialanda, and J. Blasco, Phys. Rev. B **57**, R3217 (1998).

[7] S. Yamaguchi, Y. Okimoto, H. Taniguchi, and Y. Tokura, Phys. Rev. B **53**, R2926 (1996); S. Yamaguchi, Y. Okimoto, and Y. Tokura, *ibid.* **55**, R8666 (1997).

[8] M. A. Señaris-Rodriguez and J. B. Goodenough, J. Solid State Chem. **118**, 323 (1995).

[9] T. Giarmarchi and P. L. LeDoussal, in *Spin Glasses and Random Fields*, edited by A. P. Young (World Scientific, Singapore, 1998), p. 321.

[10] B. H. Toby and T. Egami, Acta Crystallogr., Sect. A: Found. Crystallogr. **48**, 33 (1992). The multiple-scattering correction procedure for the GLAD spectrometer was carefully calibrated so that it gives a correct PDF for crystalline Ni. The same procedure is used here.

[11] S. J. L. Billinge, R. G. Difrancesco, G. H. Kwei, J. J. Neumeier, and J. D. Thompson, Phys. Rev. Lett. **77**, 715 (1996); D. Louca, T. Egami, E. L. Brosha, H. Röder, and A. R. Bishop, Phys. Rev. B **56**, R8475 (1997); D. Louca, G. H. Kwei, and J. F. Mitchell, Phys. Rev. Lett. **80**, 3811 (1998).

[12] H. D. Megaw and C. N. W. Darlington, Acta Crystallogr., Sect. A: Cryst. Phys., Diffr., Theor. Gen. Crystallogr. **31**, 161 (1975); G. Thornton, B. C. Tofield, and A. W. Hewat, J. Solid State Chem. **61**, 301 (1986); A. N. Petrov, O. F. Kononchuk, A. V. Andreev, V. A. Cherepanov, and P. Kofstad, Solid State Ionics **80**, 189 (1995).

[13] The number of Co-O pairs is determined by integration within r_1 and r_2 chosen from the beginning to the end of the first peak:

$$N_{\text{Co-O}} = \frac{4\pi\langle b\rangle \int_{r_1}^{r_2} r^2 \rho(r)\,dr}{2c_{\text{Co}} b_{\text{Co}} b_{\text{Mn}}}.$$

$\langle b\rangle$ is the average scattering length, and c is the concentration of Co atoms per unit cell.

[14] T. Saitoh, T. Mizokawa, A. Fujimori, M. Abbate, Y. Takeda, and M. Takano, Phys. Rev. B **55**, 4257 (1997).

[15] I. B. Bersuker, *Electronic Structure and Properties of Transition Metal Compounds* (Wiley, New York, 1996), p. 279.

[16] K. Asai, A. Yoneda, O. Yokokura, J. M. Tranquada, and G. Shirane, J. Phys. Soc. Jpn. **67**, 290 (1998).

[17] R. Caciuffo, D. Rinaldi, G. Barucca, J. Mira, J. Rivas, M. A. Señaris-Rodriguez, P. G. Radaelli, D. Fiorani, and J. B. Goodenough, Phys. Rev. B **59**, 1068 (1999).

[18] The determined structure function $S(Q)$ represents an integral of $S(Q)=S(Q(\omega=0))=\int_{-\infty}^{\infty} S(Q(\omega),\omega)d\omega$. If the structure is static, a change of the detector angle affects only the relation

between the time of flight and Q, leaving $S(Q)$ unaffected, so that the PDF is independent of the detector angle.

[19] T. Egami, in *Materials and Crystallographic Aspects of HT_c-Superconductivity*, edited by E. Kaldis (Kluwar Academic, Dordrecht, 1993), p. 45.

[20] D. Louca and T. Egami, Phys. Rev. B **59**, 6193 (1999).

[21] G. Placzek, Phys. Rev. **86**, 377 (1952).

[22] M. D. Kaplan and B. G. Vekhter, *Cooperative Phenomena in Jahn-Teller Systems* (Plenum, New York, 1995), p. 112.

[23] A. V. Babinskii, S. L. Ginzburg, E. I. Golovenchits, and V. A. Sanina, Pis'ma Zh. Eksp. Teor. Fiz. **57**, 289 (1993) [JETP Lett. **57**, 299 (1993)].